Collision-Induced Dissociation of Water into Ions

Igor A. Wojciechowski and Barbara J. Garrison*

Department of Chemistry, 104 Chemistry Building, Penn State University, University Park, Pennsylvania 16802

Received: August 23, 2004; In Final Form: November 24, 2004

A modification of the central force model (CFM) that describes the dissociation of water molecules into OH^- and H^+ ions is proposed for molecular dynamics simulations of energetic particle bombardment of water ice. The model keeps all the properties of the CFM but permits charge exchange between oxygen and hydrogen atoms when the water molecule starts to dissociate after collision with an energetic projectile. The reaction products, therefore, have the correct integer charges, −1 and +1 for hydroxyl and a proton. The threshold for the ionic dissociation is corrected to be at the right value, 17.2 eV, in a vacuum. Using the proposed model, total cross-sections for ionic dissociation as functions of the projectile energy are estimated for Ar and C projectiles colliding with water molecules in a vacuum and water ice. Carbon projectiles are demonstrated to produce more dissociated ions at energies lower than 300 eV. Argon projectiles are more effective in breaking the molecules at higher energies.

1. Introduction

The mechanism resulting in ion emission from solid targets during energetic ion bombardment remains elusive in a number of desorption techniques including secondary ion mass spectrometry (SIMS),[1] matrix assisted laser desorption/ionization (MALDI),[2] and electrospray ionization.[3] In these techniques, quantitative information on elemental target composition relies on the measurement of the secondary ion yield. For the special matrix of water ice, the formation mechanism and structure of ionic water clusters is of interest to researchers from different fields.[4] Ion emission from frozen samples bombarded by energetic ions is a commonly considered method for production of cluster ions of volatile liquids.[5] The energetic particle bombardment of water ice is believed to be the basis for explaining the composition of the atmospheres of some Jupiter's moons.[6]

Here we consider the ion emission process due to energetic particle bombardment as in SIMS experiments. As a model system, water has been chosen to study ionization because it is an important matrix for SIMS experiments on frozen−hydrated biological cells.[7] Ion emission from molecular solids bombarded by energetic atomic projectiles is a long-standing unsolved problem due to the variety and complexity of the processes contributing to ion formation.[8] Ions can be preformed in the original sample or be formed by energetic collisions initiating charge separation or other electronic processes. Once formed, there is the possibility of re-neutralization or decomposition into smaller species. Although molecular dynamics (MD) simulations have been successfully used to describe the motion of the neutral species due to energetic particle bombardment,[9] predicting ion formation requires a quantum mechanical treatment. Current computational approaches are not amenable for performing ab initio quantum mechanical calculations on systems containing thousands of atoms. Thus, our strategy for studying ionization is to incorporate models of individual electronic processes into the MD simulations and test the predictions with experimental data.

In the first study,[10,11] the ejection of solvated alkali and halide ions, preformed in water ice before the particle bombardment event was investigated. Significantly more cations than anions were found to emit for low initial concentrations of the ions. The cations and anions in water affect the local hydrogen bond network differently. The anions do not disrupt the network, thus making it harder for them to be ejected from the sample. The cations, however, form complexes with neighbor water molecules, breaking the hydrogen bonds. These preformed cationic clusters can more readily eject than their negatively charged counterparts. This finding was confirmed by complementary experiments,[10] where frozen water films with dissolved NaI and KI salts were exposed to a beam of 20 keV C_{60}^+ ions. The experiments reveal, however, that the major ions observed in the spectrum are the clusters associated with hydronium, hydroxyl and sometimes water ions. The initial hydronium and hydroxyl ion concentrations are presumably around 10^{-7} M. To account for these high observed signals, the ions must be formed during the collision cascade.

One of the reaction channels resulting in formation of protons and hydroxyl ions is dissociation of a water molecule into two ions as

$$H_2O \rightarrow H^+ + OH^- \qquad (1)$$

The threshold for this reaction in a vacuum, 17.2 eV, is larger, of course, than the energy of dissociation into neutral species, 5.5 eV.[12] Because the objective is to understand ion ejection, the first step is to ascertain the collision conditions that are sufficiently energetic to break the water molecules into ions, and thus dissociation into neutral species is omitted. An assumption has also been made that the Grotthuss mechanism for proton migration in water[13] does not need to be considered. This mechanism involves a well-formed hydrogen bonded network. Ion formation due to collisions, on the other hand, inherently means the atomic positions are disrupted.

In the present work, a model is proposed that allows treating collision-induced dissociation of a water molecule into two ions. Implementing the model into the MD code makes it possible to simulate the electronic effects of dissociation. Total cross-sections for ionic dissociation a function of the projectile energy

10.1021/jp046192s CCC: $30.25
Published on Web 01/20/2005

were estimated for two SIMS projectiles, Ar and C atoms, colliding with water molecules in a vacuum and water ice.

2. Model

There are only a few water models in the literature that can be used to mimic the dissociation of water into ions. The central force model (CFM) for intact water proposed by Stillinger and David[14] and its improved version by Duh, Perera, and Haymet[15] consider the water molecule as being made of three "independent" particles with bond-stretch terms, thus allowing dissociation into OH^- and H^+. To ensure a good dipole moment and correct description of other water properties, the CFM assigns fractional charges to the hydrogen atom, $q_{eH} = 0.3298$, and to the oxygen atom, $q_{eO} = -0.6596$. The products of reaction 1 must have, however, integer charges, $+1$ for the proton and -1 for the hydroxyl group, at large separations. Consequently, the model must be modified such that the charge on the atoms depends on the separation distance.

One way of controlling the charge transfer is to use the electronegativity equalization (EE) method first proposed by Sanderson[16] and developed by many authors (see the review article[17] by Rick and Stuart and references therein). Their focus was small charge fluctuations due to polarization effects in liquids. In the collision-induced dissociation environment, the primary interest is large charge transfer between two atoms. Ion separation occurs in the time scale of tens of femtoseconds, whereas the response from the sample molecules due to a changing electric field takes more than hundreds of femtoseconds.[18] The charge exchange between hydrogen and oxygen atoms, therefore, proceeds practically instantaneously within one molecule. Thus, differing from the EE method, the amount of charge transferred depends on the O−H distance and is controlled by the charge transfer function, which is assumed to be of the form[19]

$$f(r) = 1 \qquad r \le a - b$$
$$f(r) = \frac{1}{2}\left(1 - \sin\left[\frac{\pi}{2}\cdot\frac{r-a}{b}\right]\right) \qquad a - b < r < a + b \qquad (2)$$
$$f(r) = 0 \qquad r \ge a + b$$

Parameters a and b are determined by evaluating the interaction of OH^- with a bare proton using the MP4 model and the 6-311++G(3df,3pd) basis set with the Gaussian '03 code.[20] The charge exchange[21] initiates at a distance of 0.96 Å that corresponds to $r = a - b$. The charges are completely separated at a distance of 2.46 Å; that is, $r = a + b$. The charges of the hydrogen and oxygen atoms as functions of interatomic distances are given by

$$q_H(r) = q_{0H} + \Delta q_{max} f(r)$$
$$q_O(r) = q_{0O} - \Delta q_{max} f(r) \qquad (3)$$

where the reference charges, $q_{0H} = 1$ and $q_{0O} = -2$, are for the separated bare ions. The maximum charge transfer, Δq_{max}, that can be lost by the H atom and gained by the O atom in the formation of one bond is 0.6702.

Although the CFM gives the correct bulk properties of water, it gives the wrong dissociation energy for reaction 1. To obtain a more realistic potential for the dissociation energy, we construct a new function, which has the Coulombic long-range part and ensures the intermolecular interaction specific for the CFM in the bulk. The same switching function as given in eq 2 interpolates between the Coulombic long-range part $V_{Coulomb}(r)$ and the original CFM potential energy function[15] $V_{CFM}(r)$ at the distances close to the equilibrium O−H distance. The potential function for the O−H interaction now becomes

$$V_{OH}(r) = (V_{CFM}(r) - \Delta E) f(r) + V_{Coulomb}(r)(1 - f(r)) \qquad (4)$$

The constant $\Delta E = 18$ eV is fit to adjust the dissociation energy to the correct value $D_0 = 17.2$ eV in a vacuum. Parameters $a = 1.71$ Å and $b = 0.75$ Å are chosen to fit the potential energy function to the function obtained in the electron structure calculations. Total interaction energies of H_2O and OH^- as functions of the O−H separation are plotted in Figure 1. Potential functions, $V_{OH}(r)$ (eq 4) and the function taken from ref 15 to describe the H−H interaction, are used for the calculation of the total energies. The small local maximum at about 1.4 Å exists in the original CFM due to describing the H−O−H angle bend motion with a bond-stretch function.

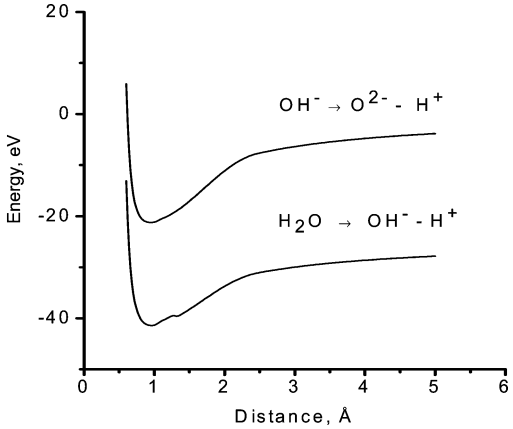

Figure 1. Total energies of H_2O and OH^- as functions of O−H separation. The CFM function is used for the H−H interaction, whereas the O−H interaction is calculated with the function as given by eq 4.

3. Dissociation Due to Collisions with C and Ar Projectiles

To understand to what extent water dissociation into the ions depends on the type and energy of the projectile, classical molecular dynamics calculations of the total dissociation cross-sections for both a water molecule in a vacuum and molecules in the water film are performed. The typical projectiles used in SIMS include Ar, Ga, and In ions as well as clusters such as SF_5, Au_3, and C_{60}. The typical incident energies are 5−20 keV per incident particle. The C_{60}^+ projectile is particularly interesting because the ion beam may be focused to a probe size of order 1 μm,[22,23] opening the possibility of greatly improved molecule-specific imaging experiments. In addition, there are suggestions that it may be possible to perform molecular depth profiling experiments[24,25] due to the low damage induced in the sample. Because there is considerable interest in C_{60} bombardment, the collision-induced dissociation due to a single C atom is considered first. Although the total energy of the C_{60} is 5−20 keV, the energy per C atom is a factor of 60 times smaller or in the range 80−300 eV. For comparison purposes, collisions with the larger Ar atom in the same energy range are performed.

The computational model and the way the simulations are conducted are described first. Then the results for C- and Ar-induced dissociation at different energies are given. Finally, the ramifications of using C and Ar projectiles for ion emission from water samples are discussed.

3.1. MD Simulations. The systems studied are a single water molecule and a slab of water ice consisting of 1056 molecules.

The interaction of C and Ar projectiles with the targets is modeled using molecular dynamics computer simulations described in detail previously.[26,27] The projectile interactions with O and H atoms are described by a pair repulsive Moliere potential with a Firsov screening length.[28]

As the charge exchange is assumed to occur only between the atoms in one molecule, the interactions were separated into inter- and intramolecular contributions. The intermolecular O−O, H−H, and O−H interaction potentials are described by the CFM functions of ref 15 adopted to have the first Coulombic term with explicitly included charges of interacting atoms.[29] For the intermolecular interaction the function given by eq 4 for the O−H interaction and the CFM H−H potential are used.

Additional forces appear in the system due to the charge exchange. They remain conservative but are no longer pairwise, because if one of two interacting particles exchanges charge with the third particle, the Coulombic forces between these two particles depend not only on their coordinates but also on the coordinates of the third particle.

The total ionic potential energy of the system reads

$$V = \sum_i \sum_{j>i} \frac{q_i q_j}{r_{ij}} = \sum_i \sum_{j>i} \left(\frac{(q_{0i} + \Delta q_i)(q_{0j} + \Delta q_j)}{r_{ij}} \right) = V_0 + \sum_i \sum_{j>i} \left(\frac{\Delta q_i q_{0j}}{r_{ij}} + \frac{\Delta q_j q_{0i}}{r_{ij}} + \frac{\Delta q_{0i} \Delta q_{0j}}{r_{ij}} \right) \quad (5)$$

where V_0 is the contribution from the constant charges, $q_{0i(j)}$ are the charges assigned to the noninteracting (isolated) particles, $\Delta q_i = -\Delta q_j = \Delta q_{max} f(r_{ij})$, and r_{ij} is the distance between ith and jth particle. Then the force acting on kth atom is the sum of three terms

$$-\vec{F}_k = \frac{\partial V_0}{\partial \vec{r}_k} + \sum_i \sum_{j>i} (q_{i0} \Delta q_j + q_{j0} \Delta q_i + \Delta q_i \Delta q_j) \frac{\partial}{\partial \vec{r}_k} \left(\frac{1}{r_{ij}} \right) + \sum_i \frac{\partial \Delta q_i}{\partial \vec{r}_k} \sum_{j \neq i} \left(\frac{q_{j0}}{r_{ij}} + \frac{\Delta q_j}{r_{ij}} \right) \quad (6)$$

The first term is calculated as usual for constant charges. The third term differs from zero only for atoms involved in charge exchange.

The total dissociation cross-section for a single molecule in a vacuum is calculated by

$$\sigma(E) = \int p(b) 2\pi b \, db \quad (7)$$

where $p(b)$ is the probability for dissociation at a given impact parameter b. The impact parameter is defined relative to the position of the oxygen atom.

The dissociation probabilities are estimated in the following procedure. For each impact parameter, which ranges from 0 to 2.0 Å in steps of 0.1 Å, a projectile is launched 1000 times. For each trajectory, the oxygen atom is placed in the origin of the coordinate system. The positions of the hydrogen atoms are set at random, oriented about the molecule's Euler angles. The reactants were initially separated by 10 Å, so that there was no interaction between them. The trajectory was stopped in 60 fs. At that time the distance between the projectile and the oxygen atom becomes more than 10 Å. The dissociation probability is simply determined as a ratio of the number of trajectories that led to dissociation to the total number of trajectories.

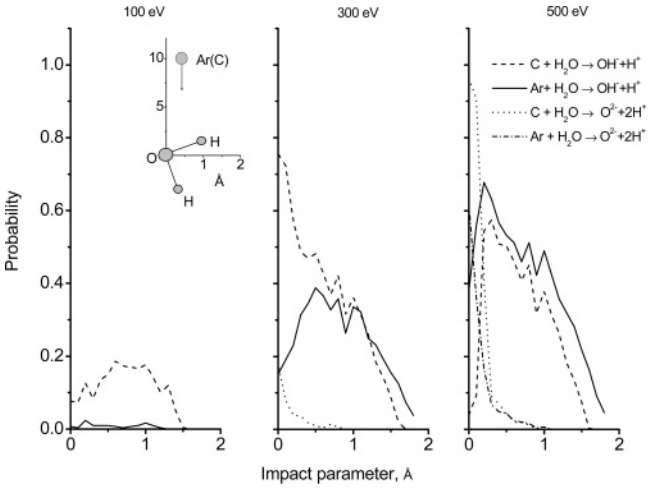

Figure 2. Probabilities of H_2O dissociation into OH^- and H^+ as well as O^{2-}, H^+, and H^+ as functions of the projectile−oxygen impact parameter for argon and carbon at three initial energies. The geometry of the system is sketched in the inset.

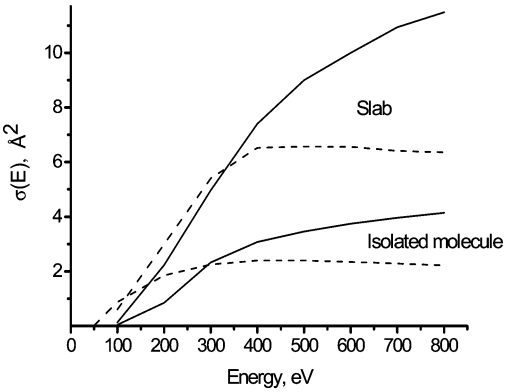

Figure 3. Total cross-sections of H_2O dissociation into the ions as functions of the projectile's energy. Solid lines are for argon; dashed lines are for carbon.

For the slab calculations, an impact area of $S = 36$ Å^2 is chosen on the surface of a 50 × 50 × 18 Å slab of water molecules. This area is occupied by six molecules. The aiming points, total number $N = 1000$ for each projectile, are chosen regularly on the area S. The original position of the projectile was 10 Å above the surface. The dissociation cross-section was determined by the formula

$$\sigma(E) = (S/6) N_d / N \quad (8)$$

where N_d is the total number of dissociated molecules. The duration of each trajectory is set to 100 fs because no more dissociation events are detected after that time.

3.2. Results and Discussion. The results of the calculations with the isolated molecule are discussed first. The probabilities of dissociation as a function of the impact parameter are plotted in Figure 2 for three energies of C and Ar, 100, 300, and 500 eV, colliding with the single molecule. Probabilities of single- and double-dissociation events, $Ar(C) + H_2O \rightarrow OH^- + H^+$ and $Ar(C) + H_2O \rightarrow O^{2-} + H^+ + H^+$, are distinguished in the plot. The total cross-sections as functions of the projectile energy, calculated with eq 7 using the probabilities of dissociation, are displayed in Figure 3. In the calculation of the cross-sections, the dissociation events are counted irrespective of whether it is single or double dissociation event. Both figures demonstrate that for projectile energies less than 300 eV, dissociation by C is more effective than that by Ar. The situation

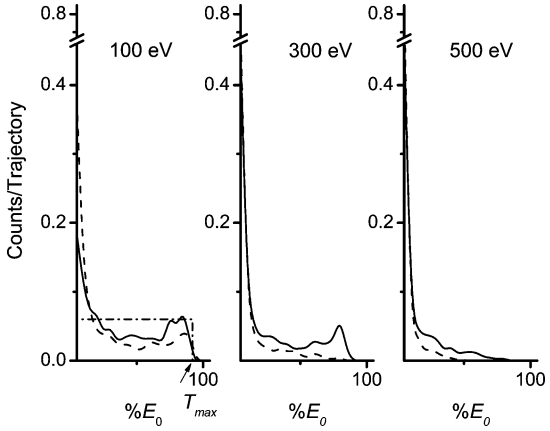

Figure 4. Kinetic energy distributions of the water molecules that survived the collision with the projectiles. Solid lines are for argon; dashed lines are for carbon. The dash−dotted line schematically shows the energy transfer cross-section for the collision of hard spheres.

changes for the energies above 300 eV, where the cross-section for C remains practically unchanged. The cross-section for Ar attains a higher value and tends to saturate at higher energies.

The reason carbon projectiles are more efficient in breaking molecules at low energies is due to the different sizes of carbon and argon atoms. For a projectile energy of 100 eV, the distance of closest approach of the C atom to the O atom is 0.7 Å, a value smaller than the O−H bond length of ∼1 Å. Consequently, the C atom can interact with the individual atom in the molecule. Collisions with either the oxygen atom (small impact parameters in the first section of Figure 2) or the hydrogen atoms (impact parameters close to unity) transfer the collision energy internally that results in dissociation. The distance of closest approach of the Ar atom to the O atom is 0.9 Å, a value comparable to the O−H bond length. The bigger argon atom tends to interact with the entire molecule rather than separately with its constituents. As a result, more energy is transferred into translation than into the internal degrees of freedom. Argon-induced dissociation at 100 eV is practically negligible. The kinetic energy distributions of the intact molecules after the collision are displayed in Figure 4 for three energies, 100, 300, and 500 eV. If the collisions between a projectile and H_2O are completely elastic, no energy is transferred internally, the distribution over the target translational energy should be approximately described by the differential energy transfer cross-section for the hard sphere potential, $\sigma = \pi R^2/T_{max}$, where R is the sum of the radii of the projectile and target. The maximum energy, T_{max}, which can be transferred to the entire molecule by both projectiles, is about 90% of the primary energy according to the formula $T_{max}/E_0 = 4m_1m_2/(m_1 + m_2)^2$. The hard sphere cross-section is schematically shown in the first section of Figure 4. The larger the deviation of the kinetic energy distribution from this constant function is the more locally the projectile interacts with the constituents, and vice versa. The least deviation is for 100 eV argon, indicating that argon transfers its energy preferably in H_2O translation. Dissociation is negligible for this case. For the energies higher than 100 eV, the distributions transform toward increasing the number of slow recoils. Consequently, the molecules remain intact only if the hydrogen and oxygen atoms get relatively small portions of the primary energy. It may happen, e.g., when the projectile is moving close to the line connecting the hydrogen atoms, comparatively far from the constituents. Collisions at smaller impact parameters with either of the constituents are accompanied by the transfer of the large amount of the collision energy internally and ultimately lead to dissociation. The increase in projectile energy, therefore, results in the Ar−H_2O interaction to become more local as it takes place for carbon at lower energies.

As seen in Figure 2, practically all the collisions between carbon and oxygen atoms become dissociative at 300 eV because the total dissociation probability, which includes single and double dissociation events, is close to unity. The probabilities of dissociation due to the collisions with the hydrogen saturate at about 0.45 for both 300 and 500 eV. They are less than unity because the hydrogen atoms are geometrically inaccessible for the projectile for some orientations of H_2O in the space. For Ar, the saturation occurs for higher energies, above 500 eV. Because the range of the Ar−H interaction is longer than that between C and H, the probability of dissociation in Ar−H collisions is larger than that in C−H collisions for all the impact parameters. Consequently, the dissociation cross-sections for Ar are larger than those for C at higher energies.

In the slab calculations, the dissociation cross-sections are larger than those for the isolated molecule (Figure 3). That is because a projectile, if it is energetic enough, can produce more than one dissociation event in a slab. Another contribution to the dissociation cross-section comes from energetic molecular recoils, H_2O molecules and OH^- groups that can break the molecules. The calculations indicate that this contribution becomes noticeable for the energies higher than 400 eV. It, of course, varies for different trajectories, but may reach as much as 35% of the total number of dissociations at 800 eV Ar. On average, Ar projectiles generate more energetic recoils than C projectiles do. For example, about 20% of H_2O recoils, generated by the 500 eV Ar projectiles, gain the kinetic energy that is greater than 250 eV, whereas only 7% of the recoils have the kinetic energy in the same region after collisions with the 500 eV C atom. For lower energies, less than 400 eV, projectile−molecule collisions are the only sources of ions in the system. The average number of dissociation events is about 1 per trajectory at 300 eV for both projectiles. This number increases twice as much for Ar at 800 eV but remaining almost the same, 1.1 per trajectory, for C at 800 eV. This larger difference between Ar and C projectiles in producing dissociation in the slab can be explained by two factors, more effective dissociation of H_2O colliding with Ar at higher energy and the fact that Ar generates more energetic recoils than C does.

3.3. Ion Emission from Water Ice. The approach proposed introduces a methodology to calculate both ion formation in water ice due to energetic particle bombardment and emission of some ions using a MD technique. This calculation is planned to be the next step in the study of ion emission from water. It would be interesting to compare the ion emission initiated by Ar and C_{60} projectiles at the same energy. Ar projectiles transfer more energy into translation of water molecules or its fragments than C projectiles do. These recoils can additionally contribute to dissociation in the film, especially for the higher projectile energies. On the other hand, carbon projectiles are more efficient in breaking water molecules into the ions than argon atoms for the initial energies below 300 eV. These energies are typical for carbon atoms constituent C_{60} projectiles, which now are of great interest for the SIMS analysis.[30] When C_{60} hits a solid surface the carbon atoms were demonstrated[30,31] not to penetrate deeply into the sample. They can generate ions in the collision cascade region near the surface. Molecules and atoms in this region with the high probability will emit into the vacuum due a large amount of the projectile's energy is deposited close to the surface. Using polyatomic projectiles can increase, therefore,

the number of emitted ions as compared to monatomic projectiles, which initiate a collision cascade deeper in the sample.[30] The question about the depth of origin of emitted ions for the two projectiles is, consequently, of large interest for the future study.

4. Conclusion

In summary, we use the original central force model for intermolecular interactions and the modified OH potential, eq 4, to describe the intramolecular interactions. For the water ice sample, the OH interaction energy is the same as in the CFM. The difference in interaction occurs when a molecule starts to dissociate. Due to the charge exchange between O and H the fractional charge on hydrogen becomes more positive (more negative on oxygen) as the separation between O and H increases. The charges are completely separated at a distance of 2.46 Å, becoming +1 for the proton and −1 for the hydroxyl group. The OH potential function was also corrected to have a right value for ionic dissociation of H_2O in a vacuum.

The estimates of the H_2O dissociation cross-sections for carbon and argon projectiles have indicated that lighter carbon at the energies less than 300 eV is more effective in breaking the molecules than argon. The situation reverses for the energies higher than 300 eV, where argon produces more ions than carbon.

Acknowledgment. The work was supported by the National Science Foundation through the Chemistry Division. The computational support was provided by Academic Services and Emerging Technologies (ASET) group at Penn State University.

References and Notes

(1) See, for example: *ToF−SIMS: Surface Analysis by Mass Spectrometry*; Vickerman, J. C., Briggs, D., Eds.; IM Publications and Surface Spectra Limited: Manchester and Chichester, 2001.

(2) See, for example: Hillenkamp, F; Karas, M.; Beavis, R. C.; Chait, B. T. *Anal. Chem.* **1991**, *63*, 1193A.

(3) See, for example: Whitehouse, C. A.; Dreyer, R. N.; Yamashita, M.; Fenn, J. B. *Anal. Chem.* **1985**, *57*, 675.

(4) Zhou, J.; Lu, X.; Wang, Y.; Shi, J. *Fluid Phase Equilib.* **2002**, *194−197*, 257.

(5) Boryak, O. A.; Stepanov, I. O.; Kosevich, M. V.; Shelkovsky, V. S.; Orlov, V. V.; Blagoy, Yu. P. *Eur. Mass Spectrom.* **1996**, *2*, 329.

(6) Johnson, R. E. *Icarus* **2000**, *143*, 429.

(7) Roddy, T. P.; Cannon, D. M., Jr.; Meserole, C. A.; Winograd, N.; Ewing, A. G. *Anal. Chem.* **2002**, *74*, 4011.

(8) Pashuta, S. J.; Cooks, R. G. *Chem. Rev.* **1987**, *87*, 647.

(9) Garrison, B. J. In *ToF−SIMS: Surface Analysis by Mass Spectrometry*; Vickerman, J. C., Briggs, D., Eds.; IM Publications and Surface Spectra Limited: Manchester and Chichester, 2001; pp 223.

(10) Wojciechowski, I. A.; Sun, S.; Szakal, C.; Winograd, N.; Garrison, B. J. *J. Phys. Chem. A* **2004**, *108*, 2993.

(11) Wojciechowski, I. A.; Sun, S.; Szakal, C.; Winograd, N.; Garrison, B. J. *Appl. Surf. Sci.* **2004**, *231−232*, 72.

(12) Dissociation energy of water into ions can be obtained from the dissociation energy of water into free radicals, 5.46 eV (Darwent, D. D. *Nat. Stand. Ref. Dat Ser. NSB* **1970**, *31*, 41), the zero point vibrational energy levels of water, 0.058 eV (Eisenberg, D.; Kauzmann, W. *The Structure and Properties of Water*; Oxford University: New York, 1969), and hydroxyl, 0.023 (Chamberlain, J. W.; Roesler, F. L. *Astrophys. J.* **1955**, *121*, 541), and the electron affinity of hydroxyl, 1.83 eV (Berry, R. S. *Chem. Rev.* **1969**, *69*, 533), as well as the ionization potential of hydrogen.

(13) Schmitt, U. W.; Voth, G. A. *J. Phys. Chem. B* **1998**, *102*, 5547.

(14) Stillinger, F. H.; David, W. *J. Chem. Phys.* **1978**, *69*, 1473.

(15) Duh, D.; Perera, D. N.; Haymet, A. D. J. *J. Chem. Phys.* **1995**, *102*, 3736.

(16) Sanderson, R. T. *Science* **1951**, *114*, 670.

(17) Rick, Steven W.; Stuart, Steven J. In *Reviews in Computational Chemisry*; Lipkowitz, K. B., Boyd, B. D., Eds.; Wiley-VCH, John Wiley and Sons, Inc.: New York, 2002; Vol. 18.

(18) Roy, S.; Bagch, B. *J. Chem. Phys.* **1993**, *99*, 9938.

(19) Tersoff, J. *Phys. Rev. B* **1988**, *38*, 9905.

(20) Frisch, M. J.; Trucks, G. W.; Schlegel, H. B.; Scuseria, G. E.; Robb, M. A.; Cheeseman, J. R.; Montgomery, J. A., Jr.; Vreven, T.; Kudin, K. N.; Burant, J. C.; Millam, J. M.; Iyengar, S. S.; Tomasi, J.; Barone, V.; Mennucci, B.; Cossi, M.; Scalmani, G.; Rega, N.; Petersson, G. A.; Nakatsuji, H.; Hada, M.; Ehara, M.; Toyota, K.; Fukuda, R.; Hasegawa, J.; Ishida, M.; Nakajima, T.; Honda, Y.; Kitao, O.; Nakai, H.; Klene, M.; Li, X.; Knox, J. E.; Hratchian, H. P.; Cross, J. B.; Adamo, C.; Jaramillo, J.; Gomperts, R.; Stratmann, R. E.; Yazyev, O.; Austin, A. J.; Cammi, R.; Pomelli, C.; Ochterski, J. W.; Ayala, P. Y.; Morokuma, K.; Voth, G. A.; Salvador, P.; Dannenberg, J. J.; Zakrzewski, V. G.; Dapprich, S.; Daniels, A. D.; Strain, M. C.; Farkas, O.; Malick, D. K.; Rabuck, A. D.; Raghavachari, K.; Foresman, J. B.; Ortiz, J. V.; Cui, Q.; Baboul, A. G.; Clifford, S.; Cioslowski, J.; Stefanov, B. B.; Liu, G.; Liashenko, A.; Piskorz, P.; Komaromi, I.; Martin, R. L.; Fox, D. J.; Keith, T.; Al-Laham, M. A.; Peng, C. Y.; Nanayakkara, A.; Challacombe, M.; Gill, P. M. W.; Johnson, B.; Chen, W.; Wong, M. W.; Gonzalez, C.; Pople, J. A. *Gaussian 03*, Revision B.05; Gaussian, Inc.: Pittsburgh PA, 2003.

(21) Wojciechowski, I. Unpublished work.

(22) Weibal, D.; Wong, S. C. C.; Lockyer, N.; Blenkinsopp, P.; Hill, R.; Vickerman, J. C. *Anal. Chem.* **2003**, *75*, 1754.

(23) Wong, S. C. C.; Hill, R.; Blenkinsopp, P.; Lockyer, N. P.; Weibel, D. E.; Vickerman, J. C. *Appl. Surf. Sci.* **2003**, *203−204*, 219.

(24) Wucher, A.; Sun, S.; Szakal, C.; Winograd, N. *Appl. Surf. Sci.* **2004**, *231−232*, 68.

(25) Sostarecz, A.; Sun, S.; Szakal, C.; Wucher, A.; Winograd, N. *Appl. Surf. Sci.* **2004**, *231−232*, 179.

(26) Garrison, B. J.; Winograd, N.; Deaven, D. M.; Reimann, C. T.; Lo, D. Y.; Tombrello, T. A.; Harrison, D. E. Jr.; Shapiro, M. H. *Phys. Rev. B* **1988**, *37*, 7197.

(27) Harrison, D. E., Jr. *CRC Crit. Rev. Solid State Mater. Sci.* **1988**, *14*, 51.

(28) Firsov, O. B. *Sov. Phys. JETP* **1958**, *6*, 534.

(29) David, C. W. *J. Chem. Phys.* **1996**, *18*, 7255.

(30) Postawa, Z.; Czerwinski, B.; Szewczyk, M.; Smiley, E. J.; Winograd N.; Garrison, B. J. *J. Phys. Chem. B* **2004**, *108*, 7831.

(31) Aoki, T.; Seki, T.; Matsuo, J; Insepov, Z.; Yamada, I. *Mater. Chem. Phys.* **1998**, *54*, 139.